Thermomechanical Modeling of Successive Material Deposition in Layered Manufacturing

R.K. Chin, J.L. Beuth and C.H. Amon
Department of Mechanical Engineering
Carnegie Mellon University
Pittsburgh, PA 15213-3890

Abstract

Residual stress build-up due to successive deposition of superheated molten metal onto metal substrates is modeled for application to layered manufacturing methods. This work is specifically applied to microcasting, which is a deposition process used within shape deposition manufacturing. One-dimensional thermal and mechanical models are used to predict temperature and stress evolution related to two physical phenomena. First, the effect of thermal cycling by newly deposited material on stress states in previously deposited and cooled layers is investigated. Here, deposited molten metal solidifies and cools to room temperature before new molten metal is deposited. For this case, predicted stress distributions as a function of depth are relatively uncomplicated and can be related to residual stress-induced part tolerance loss. In the second case, the effect of localized preheating by previously deposited material is investigated. In this model, molten metal is successively deposited at a rate comparable to that used to deposit individual droplets in the microcasting process. Results indicate that although preheating by previously deposited material strongly affects transient stresses, final stress states are not substantially altered.

Introduction

A common characteristic of many layered manufacturing methods is the successive deposition of molten material. In such processes, the subsequent solidification and cooling of deposited material leads to differential thermal strains and the build-up of residual stress. Undesirable effects of residual stresses can include part warping, loss of edge tolerance and delamination between deposited layers. In parts subjected to applied loads, residual stress can also reduce apparent strength and service life. Ultimately, in order to control the undesirable effects of residual stresses through process changes and part design changes, it is necessary to understand how such stresses build up during manufacture.

Although the problem of residual stress build-up is inherent in any process involving successive deposition of molten material, attention is focused in this paper on modeling stress evolution in shape deposition manufacturing (SDM). SDM is distinct from other layered manufacturing processes in that it aims to directly build fully dense, functional metal parts to machined tolerances (Merz et al., 1994). After each layer is deposited, it is machined to specified dimensions prior to deposition of the next layer. Other processing operations, such as shot peening, can also be incorporated into the manufacture of a part. Within SDM, a process for depositing layers is required. The principal deposition process currently in use is termed microcasting, in which large (1-5 mm in diameter) droplets of molten material are deposited onto existing material which is at or near room temperature.

The goal of this work is to model successive deposition of superheated molten metal onto a metal substrate. In the next section, one-dimensional thermal and mechanical models are described which are used to study material deposition at two rates. Results are then presented for the case of material deposition occurring at a slow rate, such that existing material has reached a uniform room temperature before new material is deposited. These results are used to investigate how mechanical stress states in existing layers of material are altered by the deposition of newly applied layers. A second set of results is then presented for the case of material deposition occurring at a rate comparable to that at which droplets are deposited during microcasting. These results are used to

examine the thermal issue of localized preheating by previously applied droplets and the effect of this preheating on residual stresses.

Model Description

Figure 1 shows a schematic of the one-dimensional thermal and mechanical models used in this study. The models consist of a substrate which is 12.7 mm thick and five deposited layers, each having a thickness of 0.8125 mm. These dimensions match substrate and droplet thicknesses typical for microcasting. The thermal model used is explicitly one-dimensional and the mechanical model used is axisymmetric, with appropriate boundary conditions used to render the stresses at any time a function of the axial (z) coordinate only.

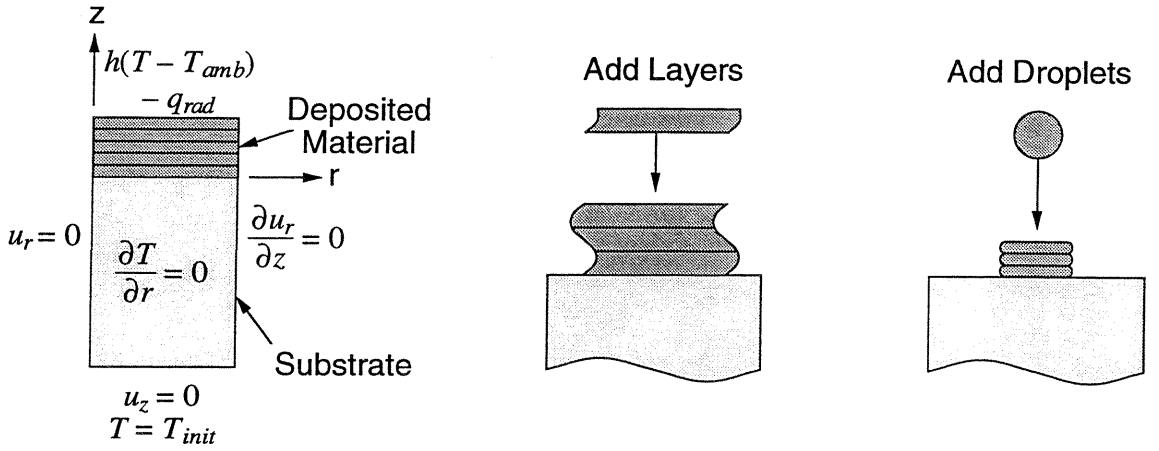

Figure 1. Thermal and Mechanical Models and Physical Problems Studied

The approach used in this study is to first obtain a thermal solution and to then use the temperature solution as an input to the mechanical model. In the mechanical model, loading is caused by differential thermal strains. Mechanically induced temperature changes are assumed to be negligible. The ABAQUS finite element package is used with thermal elements and stress elements having a quadratic interpolation of temperatures and displacements. The mesh resolution in the z direction is the same for each of the models. The thickness of each deposited layer is discretized by 10 elements of equal size and the substrate contains 18 elements through its thickness. The substrate mesh is strongly biased toward the top of the substrate. In this study, the deposition of medium carbon steel onto a medium carbon steel substrate is examined.

In the thermal model, boundary conditions modeling convection to the surroundings and radiation from a heat source (the welding torch for melting feedstock wire to create droplets) are imposed on the top surface of the newly deposited layer (Fig. 1). The convection heat transfer coefficient, h, is specified as 5.3 W/m^2-K, the ambient temperature, T_{amb}, is 323 K and the radiation heat flux, q_{rad}, is specified as 2092 W/m^2. The ambient temperature is higher than room temperature because of the nearby heat source. These temperatures and thermal properties follow those used by Amon et al. (1996). Initial temperatures used in the model are 2573 K for the molten material (which is typical for microcasting of carbon steel) and 303 K (room temperature) for the substrate. At the bottom of the substrate, a fixed temperature equal to the initial temperature is imposed. The temperature-dependent thermal conductivity, specific heat and diffusivity used are based on data from Allard (1969) and Touloukian (1967) and are applicable to a low to medium carbon steel. The carbon steel is modeled as having a liquidus temperature of 1770 K, a solidus temperature of 1716 K and a latent heat of fusion of 272 kJ/kg.

In the mechanical model the top of the droplet is traction-free, with no imposed displacement constraints (Fig. 1). The centerline is constrained to have zero radial displacement,

while the outer wall is constrained to expand (or contract) uniformly in the radial direction. A condition of zero axial (z) displacement is applied at the bottom of the model. Because this model maintains straight vertical edges and a flat substrate bottom, deposition under the constraint of no bending deformation is modeled. In the microcasting process, parts are built on a large pallet which is very stiff in bending. Because the right edge of the model is free to expand or contract uniformly, the net radial force equals zero. These boundary conditions and the absence of radial temperature variation lead to a biaxial stress state $\sigma_{rr}(z) = \sigma_{\theta\theta}(z)$ with all other stresses equal to zero. The stress distribution at any time is therefore fully described by a plot of σ_{rr} vs. z.

The temperature-dependent Young's modulus used in the mechanical model is from data of Thomas et al. (1987), while the temperature-dependent linear thermal expansion coefficient is taken from the *ASM Metals Reference Book* (1981). To account for time-dependent creep deformation, a secondary (steady-state) creep law for a medium carbon steel in the austenitic phase is used. It is given by Thomas et al. (1987) as

$$\dot{\varepsilon} = A(\sinh(B\sigma))^n \exp\left(-\frac{C}{T}\right), \qquad (1)$$

where $\dot{\varepsilon}$ = equivalent creep strain rate in seconds^{-1}
σ = Mises equivalent stress in MPa
T = temperature in K
A = 907×10^{10}
B = 0.0356
C = 41938
n = 6.9

In this study, time-independent plasticity is not modeled. Through its stress dependence, however, the creep law in (1) approximately models temperature-dependent yielding without strain hardening. For example, at room temperature (303 K), a stress of 400 MPa results in a strain rate of 2.8×10^{-7}/s. As the stress is increased, the strain rate increases significantly. For example, at a stress of 430 MPa the strain rate equals 5.1×10^{-3}/s. Because a strain rate of 2.8×10^{-7}/s will result in insignificant stress relaxation under displacement controlled conditions, 400 MPa is a reasonable definition for an effective yield stress at room temperature based on the creep law in (1).

The thermal and mechanical models described above can be used to examine two types of physical problems, which are illustrated in Fig. 1. First, these models can be used to simulate temperature and stress evolution for the deposition of entire layers onto existing layers of a part and the substrate it is built upon. The results would be exact for the case of a part with insulated sides and with free edges constrained to displace uniformly in the radial direction, but they are also reasonable away from the free edges in a part built to be constrained from bending deformation. In relating this type of model to microcasting, effects associated with the drop-by-drop deposition of individual layers are neglected; however, such a model can give insight into how stresses develop on a layer level. Second, as noted in Chin, Beuth and Amon (1996), the thermal and mechanical models schematically illustrated in Fig. 1 can also be used to approximate conditions near the centerline of deposited droplets, where each droplet has a height that is small compared to its radius. For such droplet geometries, the radial displacement becomes increasingly uniform in the z direction and the heat transfer into the substrate becomes increasingly axial as the centerline is approached.

Recognizing the two physical interpretations outlined above, thermal and mechanical models are used in this paper to study two cases which differ in deposition rate. In the first case (related to the first physical interpretation), existing material is allowed to cool to room temperature before new material is deposited. Results from this modeling are used to investigate how deposition of new material layers alters residual stress states in existing layers. In the second case, new material is deposited onto material that has not had time to cool to room temperature, at a rate comparable to that used to deposit droplets in the microcasting process. Results from this

modeling are used to investigate how local preheating due to a previously deposited droplet affects stress evolution in droplets deposited on top of it. Although microcast droplets are typically deposited adjacent to each other, these results provide insight into multiple droplet deposition without having to resort to three-dimensional modeling. In both cases, deposition is onto a substrate that is initially stress-free and at room temperature.

Transient Results

In this section, transient temperature and stress results are presented for successive deposition of two layers or droplets of carbon steel onto a carbon steel substrate. Results for deposition of succeeding layers or droplets show similar trends. In the next section of this paper, final stress results are presented for the deposition of a total of five layers or droplets.

Slow Deposition

For the case of a slow rate of material deposition, Figs. 2 and 3 illustrate transient temperature and radial stress distributions due to deposition of a first layer of superheated carbon steel onto a stress-free room temperature carbon steel substrate. In the figures, temperatures and stresses are plotted as a function of the axial (z) coordinate at discrete times. An axial coordinate of zero represents the location of the interface between the substrate and the deposited material. The substrate has a negative coordinate and the deposited material has a positive coordinate.

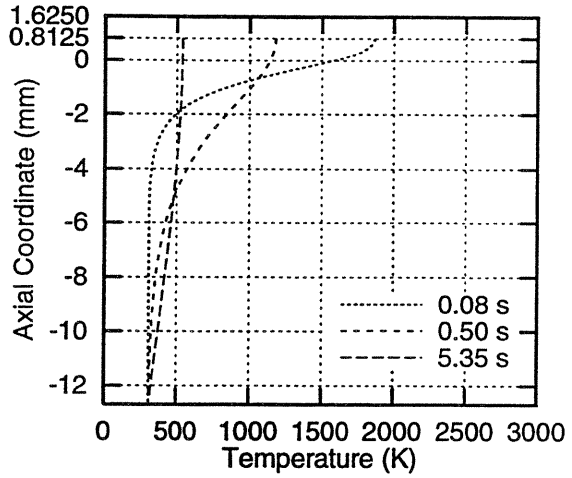

Figure 2. Transient Temperatures for Deposition of a Single Layer

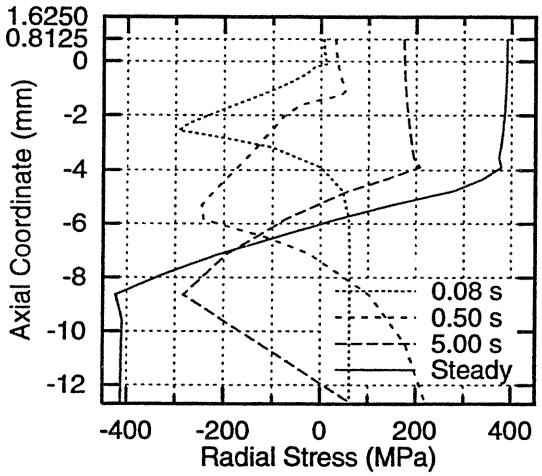

Figure 3. Transient Radial Stresses for Deposition of a Single Layer

As shown in Fig. 2, heat conducted from the molten material into the substrate initially raises the temperature of the top portion of the substrate hundreds of degrees K (see t = 0.08 s). Because this high temperature region is constrained against free expansion by the remainder of the substrate, this leads to compressive stresses (Fig. 3). As shown by the plot for t = 0.08 s in Fig. 3, inelastic straining occurs while the substrate is under compression at elevated temperatures, limiting the magnitude of the compressive stresses at the very top of the substrate. After the substrate material reaches its maximum temperature, which differs for each location, it begins to cool but is constrained from freely contracting. As this happens, the stress state in the top of the substrate turns from compression to tension (see Fig. 3 at t = 0.50 s and t = 5.00 s). To maintain zero net radial force, the stresses in the bottom of the substrate become compressive. Tensile stresses build up in the deposited layer due to constrained thermal contraction, but their magnitude at early times is limited by stress relaxation due to high temperature creep. As the temperature decreases further, the combination of further constrained thermal contraction and a diminished role of creep deformation increases the magnitude of tensile stresses in the layer. The final stress state consists of tensile stresses of large magnitude (near yield) in the deposited layer, which also extend to a depth of approximately 5 layer thicknesses into the substrate. The time to reach a steady-state

thermal condition, defined in this study as the time it takes for all portions of the model to be at or below 307 K, is approximately 30 seconds.

In the slow deposition rate simulations, layer 2 is deposited after both layer 1 and the substrate cool to steady state. Except for the effect of the addition of the thickness of the first deposited layer to the thickness of the substrate, thermal results for deposition of the second layer are identical to those for deposition of the first layer (Fig. 2). Therefore the transient temperature distributions for additional layers are not shown.

Figure 4 provides plots of radial stress as a function of the axial coordinate, z, at discrete times during deposition of a second layer. The initial stress distribution in the substrate and first layer is simply the final stress distribution shown in Fig. 3. In Fig. 4 it is evident that at early times (see data for t = 0.08 s), heat from the newly deposited second layer conducts into the first layer and the top of the substrate, relieving the large residual tensile stresses there and placing this region into compression. The compressive stresses do not extend as deeply into the existing material as they do at a similar time in Fig. 3. At later times, however, stress distributions in Fig. 4 become increasingly similar to those in Fig. 3. At steady state, the stress distribution is almost identical to the steady-state stress distribution shown in Fig. 3, with a similar tensile zone present in the deposited material and the top of the substrate. The tensile zone has moved upward slightly, however, compared to that in the initial stress distribution. Thus, although the initial stress state present in depositing a second layer alters stress distributions at early times, the final stress distributions are only slightly different.

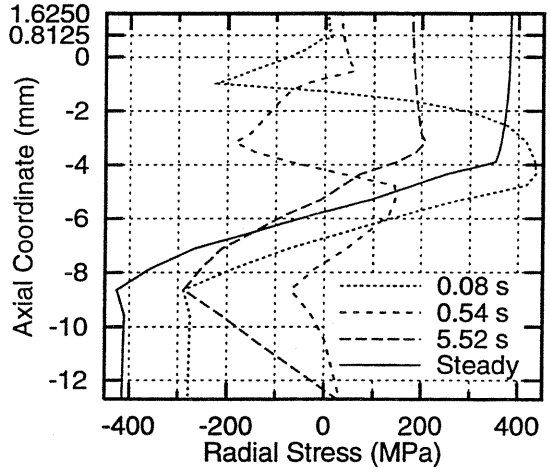

Figure 4. Transient Radial Stresses for Slow Deposition of a Second Layer

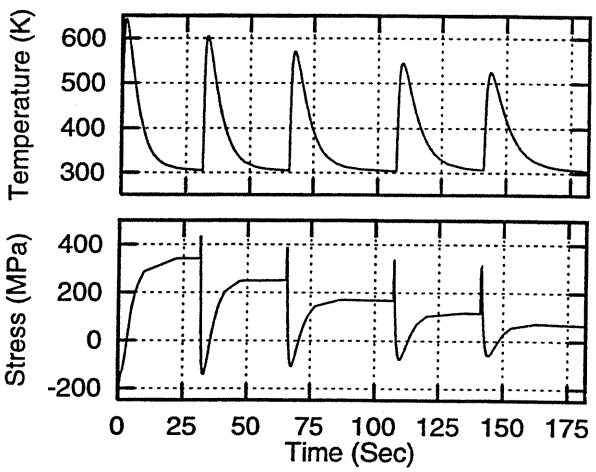

Figure 5. Temperature and Radial Stress at z = -4.34 mm (Slow Rate)

Another way to consider the transient behavior for the case of a slow rate of material deposition is to examine the history of temperature and radial stress at a particular point. This type of result is illustrated in Fig. 5 for a history point located approximately five layer thicknesses into the substrate, at a depth of 4.34 mm. The sharp peak in radial stress near t = 30 s in Fig. 5 corresponds to the maximum stress in Fig. 4 near z = -4 mm at a time of 0.08 seconds after the second layer is deposited. This peak in radial stress is brought about as a reaction to the compressive stress initially induced in the top of the substrate, due to the model requirement of no net force in the radial direction. This maximum in tensile radial stress, (and the compressive stresses in the top of the existing material that cause it) occurs over a very short period of time. The other sharp peaks in radial stresses in Fig. 5 correspond to similar maxima which occur after each succeeding layer is deposited. The periodic behavior observed in radial stresses is also seen in the temperature results plotted in Fig. 5. Temperatures rise rapidly after each layer is deposited,

due to conduction of heat from newly deposited material to the history point. The coinciding constrained thermal expansion results in compressive radial stress.

Rapid Deposition

For the case of a rapid rate of material deposition, material is deposited every 0.50 seconds, which is comparable to the rate at which droplets are deposited in the microcasting process. These simulations begin in the same manner as for slow deposition; however, 0.5 seconds after deposition of the first droplet, the existing distribution of temperature and stress is taken as the initial condition for deposition of the second droplet. After another 0.5 seconds, a third droplet is deposited and this procedure is repeated until the modeling of all droplet deposition is complete.

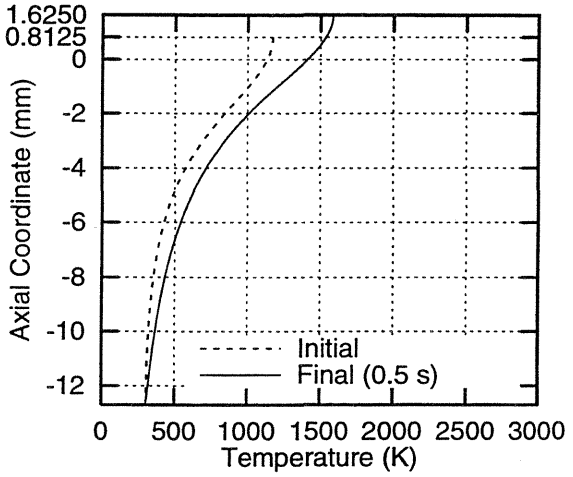

Figure 6. Transient Temperatures for Rapid Deposition of a Second Droplet

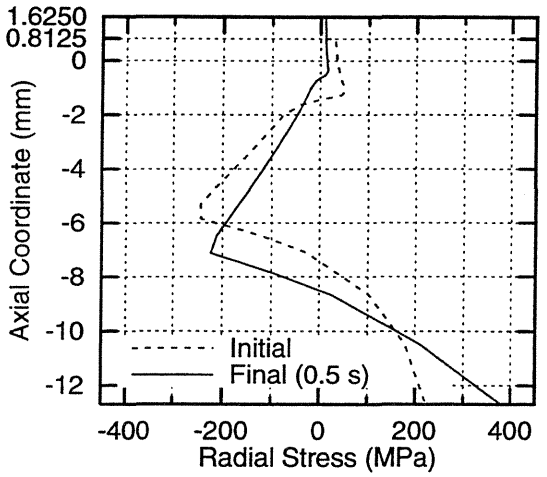

Figure 7. Transient Radial Stresses for Rapid Deposition of a Second Droplet

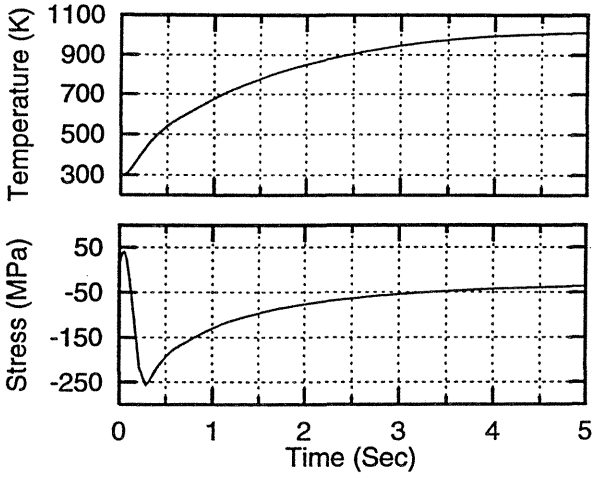

Figure 8. Temperature and Radial Stress at z = -4.34 mm (Rapid Rate)

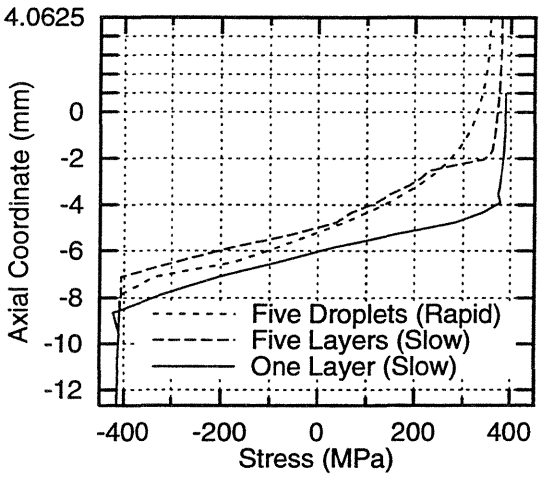

Figure 9. Final Radial Stress Distributions for Slow and Rapid Deposition

Figures 6 and 7 show the initial and final (after 0.50 s) distributions of temperature and stress due to deposition of a second droplet of material. Initial and final temperature and stress distributions are not substantially different and results are not plotted for other times because the distributions do not change substantially over the 0.50 seconds of the simulation. The first droplet and top portion of the substrate do experience an overall increase in temperature, however, due to heat conducted from the newly applied material.

In Fig. 8, results are plotted that are analogous to those plotted in Fig. 5, at the same location of z = -4.34 mm. The behavior is substantially different than that shown in Fig. 5, however. For the case of rapid material deposition, oscillations in temperature and radial stress are not apparent after the first droplet is deposited. Instead, as was noted in the results of Fig. 6, the addition of heat from newly applied material causes the temperature at this location to steadily rise. The compressive stress seen in Fig. 8 is a reaction to the tensile stresses in the top of the substrate and the deposited droplets. These stresses decrease primarily because increasing temperatures in the top portion of the model cause the tensile stresses there to be relieved due to creep. However, temperatures at the location z = -4.34 mm also become high enough to allow direct relaxation of the compressive stress.

Final Stress States

In this section, final states of stress are presented for the cases of slow and rapid deposition of superheated carbon steel onto an initially stress-free carbon steel substrate at room temperature. Deposition of a total of five layers or droplets is modeled and results are presented at a time after the last deposited material cools to room temperature. Figure 9 compares these results with the steady-state stress distributions due to the deposition of a single layer of material (the final stress state given in Fig. 3). The most striking characteristic of the plots provided in Fig. 9 is that they are not substantially different, despite the range of material deposition rates modeled and the different transient behavior observed. Also, all three plots show relatively simple residual stress distributions despite the complicated transient thermal and stress cycling that the material undergoes during the deposition process. It should be restated, however, that current material modeling does not include strain hardening. If hardening were included, the uniformity of stress states seen in Fig. 9 would be diminished.

During slow deposition, the small upward translation of the tensile zone observed in Fig. 4 after the second layer reaches steady state also occurs upon deposition of succeeding layers. The final stress distribution thus has the appearance of the stress distribution after deposition of a single layer, but with the tensile zone shifted upward. Also, the depth of the tensile zone is greater than that due to deposition of a single layer.

Separation of a part from the substrate upon which it is built will, in general, relieve a net residual force and bending moment in the deposited material, resulting in tolerance losses through part warping and contraction. In the building of parts by layered manufacturing, part warping is a significant concern because it can lead to substantial loss of dimensional tolerance. In the simulations presented here, however, a part separated from the substrate will contract, but not warp because there is essentially no net moment in the deposited material. For other configurations (e.g., different layer thicknesses), the same conclusion applies if the deposited material remains in the region of essentially uniform tension in the upper half of the deposited part and substrate.

The plot of final stresses for the case of rapid material deposition is similar to that for the case of slow material deposition; however, the tensile stress magnitudes are slightly lower. This is due to nonuniform preheating of the top portion of the existing material by prior droplets. The magnitude of the stress reduction is not large. A much larger reduction in residual stress magnitudes is indicated in simulations of uniform substrate preheating (Chin, Beuth and Amon, 1995, 1996).

Conclusions

In this paper results are presented for one-dimensional modeling of successive material deposition at two deposition rates. Results for a slow rate of deposition are related to the physical problem of successive deposition of material layers to build a part, providing insight into how residual stresses in existing material are affected by deposition of succeeding layers. Results for a rapid rate of deposition are related to the problem of successive deposition of molten droplets,

giving insight into how localized preheating by previously deposited droplets affects residual stress distributions.

Results for a slow rate of deposition suggest that existing stress states in previously deposited material do not significantly change final stresses compared to deposition on a stress-free substrate. Residual stress magnitudes in a deposited part can be large during deposition; however, these stresses are relaxed upon release of the part from the substrate it is built upon. The final stress state in the deposited material is essentially uniform biaxial tension. For such stress states, the deposited material will become essentially stress-free upon separation from the substrate, with a net contraction but no warping deformation. Results for a rapid rate of deposition indicate that preheating by previously deposited droplets alters transient temperature and stress distributions and increases the average temperature in the existing material. This preheating does not significantly reduce final stresses, however. This issue will be further explored through three-dimensional modeling of successive deposition of adjacent droplets. Overall, only minor differences in final stress states are observed over the range of deposition rates studied.

Acknowledgments

The authors gratefully acknowledge financial support from the Carnegie Mellon University Department of Mechanical Engineering and the National Science Foundation under Grants CMS-9411005, CTS-9311072 and DMI-9415001. The authors would also like to thank Lee Weiss and Fritz Prinz for their insights related to the application of this work to shape deposition manufacturing.

References

Allard, S. (ed.) (1969). Metals thermal and mechanical data, Metaux donnees thermiques et mecaniques. *Tables internationales de constantes selectionnees 16*, Oxford, New York, Pergamon Press.

Amon, C.H., Schmaltz, K.S., Merz, R. and Prinz, F.B. (1996). Numerical and experimental investigation of interface bonding via substrate remelting of an impinging molten metal droplet. *Journal of Heat Transfer 118*, in press.

ASM Metals Reference Book: A handbook of data about metals and metalworking (1981). Compiled by The Editorial Staff, Reference Publications, American Society for Metals, 167.

Chin, R.K., Beuth, J.L. and Amon, C.H. (1995). Control of residual thermal stresses in shape deposition manufacturing. *Proc. 1995 Solid Free-form Fabrication Symposium*, H.L. Marcus, J.J. Beaman, D.L. Bourell, J.W. Barlow and R.H. Crawford eds., Austin, August 1995, 221-228.

Chin, R.K., Beuth, J.L. and Amon, C.H. (1996). Thermomechanical modeling of molten metal droplet solidification applied to layered manufacturing. Submitted to *Mechanics of Materials*.

Merz, R., Prinz, F.B., Ramaswami, K., Terk, M. and Weiss, L.E. (1994). Shape deposition manufacturing. *Proc. 1994 Solid Free-form Fabrication Symposium*, H.L. Marcus, J.J. Beaman, D.L. Bourell, J.W. Barlow and R.H. Crawford eds., Austin, August 1994, 1-8.

Thomas, B.G., Samarasekera, I.V. and Brimacombe, J.K. (1987). Mathematical modeling of the thermal processing of steel ingots: part II. stress model. *Metallurgical Transactions B 18B*, 131-147.

Touloukian, Y.S. (ed.) (1967). *Thermophysical Properties of High Temperature Solid Materials*, Macmillan, New York.